GeoHealth

RESEARCH ARTICLE
10.1029/2021GH000568

Special Section:
The COVID-19 pandemic: linking health, society and environment

Lower COVID-19 Incidence in Low-Continentality West-Coast Areas of Europe

Karin Ebert[1], **Renate Houts**[2], **and Sergio Noce**[3]

[1]Natural Sciences, Technology and Environmental Studies, Södertörn University, Stockholm, Sweden, [2]Department of Psychology and Neuroscience, Duke University, Durham, NC, USA, [3]Fondazione Centro Euro-Mediterraneo sui Cambiamenti Climatici (CMCC), Division on Impacts on Agriculture, Forests and Ecosystem Services (IAFES), Viterbo, Italy

Key Points:

- We study the reason for within country differences of the COVID-19 pandemic for Norway, Sweden, Germany, Italy, and Spain
- COVID-19 incidence is lower in climate zones with smaller annual temperature ranges and a clear division between wet and dry seasons
- Incidence patterns can be explained by continentality; oceanic impact limits COVID-19 at open west coasts in the European west wind zone

Supporting Information:

Supporting Information may be found in the online version of this article.

Correspondence to:

K. Ebert,
karin.ebert@sh.se

Citation:

Ebert, K., Houts, R., & Noce, S. (2022). Lower COVID-19 incidence in low-continentality west-coast areas of Europe. *GeoHealth*, *6*, e2021GH000568. https://doi.org/10.1029/2021GH000568

Received 27 NOV 2021
Accepted 11 APR 2022

Author Contributions:

Conceptualization: Karin Ebert
Data curation: Karin Ebert
Formal analysis: Karin Ebert, Renate Houts, Sergio Noce
Investigation: Karin Ebert
Methodology: Karin Ebert, Renate Houts, Sergio Noce

Abstract In March 2020, the first known cases of COVID-19 occurred in Europe. Subsequently, the pandemic developed a seasonal pattern. The incidence of COVID-19 comprises spatial heterogeneity and seasonal variations, with lower and/or shorter peaks resulting in lower total incidence and higher and/or longer peaks resulting higher total incidence. The reason behind this phenomena is still unclear. Unraveling factors that explain why certain places have higher versus lower total COVID-19 incidence can help health decision makers understand and plan for future waves of the pandemic. We test whether differences in the total incidence of COVID-19 within five European countries (Norway, Sweden, Germany, Italy, and Spain), correlate with two environmental factors: the Köppen-Geiger climate zones and the Continentality Index, while statistically controlling for crowding. Our results show that during the first 16 months of the pandemic (March 2020 to July 2021), climate zones with larger annual differences in temperature and annually distributed precipitation show a higher total incidence than climate zones with smaller differences in temperature and dry seasons. This coincides with lower continentality values. Total incidence increases with continentality, up to a Continentality Index value of 19, where a peak is reached in the semicontinental zone. Low continentality (high oceanic influence) appears to be a strong suppressing factor for COVID-19 spread. The incidence in our study area is lowest at open low continentality west coast areas.

Plain Language Summary In March 2020, the first known cases of COVID-19 occurred in Europe. Over the next 16 months (March 2020 to July 2021) a pattern emerged where some areas had higher versus lower COVID-19 spread. We studied whether this pattern could be explained by climatological factors in five European countries (Norway, Sweden, Germany, Italy, and Spain). Our results show that areas with larger annual temperature ranges and year-round rain had higher COVID-19 spread than areas with smaller annual temperature ranges and dry seasons. We also examined continentality, which measures the influence of the ocean on climate. In Europe, where predominant winds come from the west, we find the highest oceanic influence at open west coasts; in our study area these are represented by north-west Spain, northernmost Germany, and south-west Norway. In these areas, COVID-19 spread was lowest. With decreasing oceanic influence, COVID-19 spread was higher. For the five countries we studied, we found highest COVID-19 spread in south-east Norway, the entire south of Sweden, the south-eastern part of Germany, northern Italy, and central Spain. Healthcare decision makers in areas that have wide ranges of temperature and rain throughout the year or that have little oceanic influence should expect a higher COVID-19 spread.

1. Introduction

In March 2020, the first known cases of the COVID-19 pandemic, caused by the respiratory virus SARS-CoV-2, occurred in European countries (JHUM, 2020; Ritchie et al., 2020). Since that time, scientists from many fields have been trying to understand conditions that lead some areas to have rampant COVID-19 outbreaks while other areas are spared. Identifying which areas have higher versus lower overall COVID-19 spread and unraveling factors that differ between them can help health care decision makers to better understand and prepare for future waves of the pandemic. In this study, we examine how two environmental factors, Köppen-Geiger climate zones and the Continentality Index, relate to total COVID-19 incidence between March 2020 and July 2021 in municipalities and counties in 5 European countries (Norway, Sweden, Germany, Italy, and Spain) while statistically controlling for crowding.

Project Administration: Karin Ebert
Resources: Karin Ebert, Renate Houts, Sergio Noce
Software: Karin Ebert, Renate Houts, Sergio Noce
Supervision: Karin Ebert
Validation: Karin Ebert, Renate Houts, Sergio Noce
Visualization: Karin Ebert
Writing – original draft: Karin Ebert, Renate Houts, Sergio Noce
Writing – review & editing: Karin Ebert, Renate Houts, Sergio Noce

Meteorological and climatic (meteoclimatic) conditions are known to have a strong correlation with pneumonia diseases (Bull, 1980; D'Amato et al., 2014; Shaman & Kohn, 2009; Tamerius et al., 2013). Particularly, climatic parameters that act on a large-scale level to influence the COVID-19 pattern have been discussed in literature; these include humidity and temperature (Byun et al., 2021; Chen, Jia, Han, 2021; Chen, Prettner, et al., 2021; Loché Fernández-Ahúja & Fernández Martínez, 2021; Matthew et al., 2021; Notari, 2021) and the intensity of variations in temperature (Kronfeld-Schor et al., 2021; Piazzola et al., 2021). For example, in New York, USA, days with a higher minimum temperature, a higher average temperature, or poorer air quality were associated with higher daily reported COVID-19 cases (Bashir et al., 2020). Other studies have focused on maritimity (Piazzola et al., 2021) or the closeness to the equator (Chen, Jia, Han, 2021; Chen, Prettner, et al., 2021), with the general finding that a mild and humid climate appears to suppress COVID-19 cases. Nonetheless, results are contradictory, likely because many studies were carried out using data from the first months of the pandemic when incidence patterns were still emerging. Further work is necessary using longer term data to understand how meteoclimatic conditions impact the spread of COVID-19.

We test whether differences in the total incidence of COVID-19 across 16-months within countries can be explained by two environmental factors: the Köppen-Geiger climate zones and the Continentality Index. Köppen-Geiger (Beck et al., 2018; Geiger, 1954; Köppen, 1900; Kottek et al., 2006) is a quantitative bioclimatic classification based on temperature and rainfall and their distribution throughout the year. This classification is widely used to examine phenomena such as the effect of climate change (Cui et al., 2021; Santini & di Paola, 2015), the impact of El Nino (Naranjo et al., 2018), or the impact of climate on human-health (e Almeida et al., 2020; Yang & Matzarakis, 2016). The Continentality Index (Conrad, 1945; Driscoll & Yee Fong, 1992), a measure of how much temperature varies within a year, has been shown to relate to human health in various studies (Ben-Ahmed et al., 2009) and to respiratory diseases due to pollen allergy (Rojo et al., 2021). Köppen-Geiger climate zones and Continentality Index are both climatic descriptors characterizing the average climatic conditions of a given area. Since they refer to long periods of time (about 30 years), they are more useful when comparing different geographical regions, as we attempt to do, than are purely meteorological indices that describe local and very short-lasting events.

Comparing COVID-19 incidence across geographical regions presents several challenges. First, the measure of COVID-19 incidence must be comparable across geographical regions for the time period studied. Luckily, the incidence of the confirmed SARS-CoV-2 occurrence per 100 k inhabitants is commonly used in European countries to express the status of the COVID-19 pandemic (ECDC, 2020). Countries typically report 2 incidence metrics: (a) the 7-day added or average values per day that can be used to describe the temporal pattern of COVID-19 cases over time, and (b) the total incidence that gives the cumulative value of known cases over the time period chosen. Examining daily patterns indicates that, like other respiratory viruses (e.g., Influenza and Respiratory Syncytial Virus), COVID-19 spreads with probable seasonality (Bloom-Feshbach et al., 2013; Byun et al., 2021; Choi et al., 2021; Liu et al., 2021; Obando-Pacheco et al., 2018). Seasonal patterns with lower and/or shorter peaks result in lower total incidence, while seasonal patterns with higher and/or longer peaks result in higher total incidence. By studying total incidence over a full-year cycle, we account for the variation in seasonal fluctuations in COVID-19 that do not necessarily happen at the same time in all geographic regions. At least a full year is needed for our purposes because climate zones and continentality act differently locally but have a summarized long-term impact. Here, we analyze the total incidence from the beginning of the pandemic in March 2020 over a more than full year circle to mid-July 2021. This time period includes the smaller first wave in spring 2020 (with low test rates), but especially, the two larger waves that followed, during autumn/winter 2020/2021 and during spring 2021.

Second, the COVID-19 incidence measures must correspond to the geographic regions used for the environmental factors we study. We know that COVID-19 incidence varies within countries and that countries also have multiple climate zones and varying continentalitiy within their borders. We therefore investigate the pattern of the total incidence and environmental factors within the smallest spatial entities (municipalities and counties) for which data were available in our countries of interest.

Finally, factors that could potentially confound the hypothesized relationships between total COVID-19 incidence and environmental factors must be taken into account. Specifically, COVID-19 cases have been shown to amplify in crowded urban areas (Rader et al., 2020). This has been explained with various hypotheses such as a greater concentration of air pollutants in areas with a greater urban vocation (Martelletti & Martelletti, 2020) or

simply because the greater the degree of urbanization, the greater the possible social interactions between people (Sharmeen et al., 2014). We therefore chose to use the degree of urbanization (Dijkstra et al., 2020) provided by the European Commission (Florczyk et al., 2019) as a control measure in all of our analyses.

In summary, we examine how two environmental factors relate to total COVID-19 incidence between March 2020 and July 2021 in five countries (Norway, Sweden, Germany, Italy, and Spain) that represent a European north-south and east-west cross-section through climate zones and continentality, and where data are available for county or community-sized entities.

2. Method

We use a combination of Geographic Information Systems (GIS) (ArcGIS Pro v2.8) and regression and analysis of variance (SAS v9.4) to investigate the relationships between COVID-19 incidence and two environmental factors (climate zones and continentality), while controlling for the degree of urbanization. Geographic Information Systems (GIS) is a long-used tool in health related studies and has been used to support spatial decisions in health care services (McLafferty, 2003), for health surveillance (Luan & Law, 2014), and to access environmental health determinants (Nordbø et al., 2018). Geographic Information Systems (GIS) has been used as a tool to investigate COVID-19 from the very beginning of the pandemic (Franch-Pardo et al., 2020; Kamel Boulos & Geraghty, 2020), mostly for dashboard mapping (cf. JHUM, 2020). Even though mapping of risk or correlations is advancing (e.g., Al-Kindi et al., 2020; Hassaan et al., 2021) the potential of GIS as a helping tool to understand COVID-19 is far from being fully utilized (Ahasan & Hossain, 2021). We here integrate GIS and statistics to find both a (visualized) pattern and statistical correlations between COVID-19 and environmental factors.

For the GIS visualization and analysis of municipalities and counties, we use the *Nomenclature des Unités Territoriales Statistiques* (NUTS) data sets, *Nomenclature des Unités Territoriales Statistiques* (NUTS3) (counties) for Spain, Italy, and Germany and *Nomenclature des Unités Territoriales Statistiques* (NUTS) communes for Sweden and Norway (Eurostat, 2020).

We imported the total incidence for each county/commune (municipality), from official sources where these data were available, with incidence data for Sweden (Folkhälsomyndigheten, 2021); Norway (VG, 2021); Germany (Robert Koch Institut, 2020); Italy (Github, 2021); and Spain (CNECovid, 2021).

Köppen-Geiger climate zones were assigned to each county/commune, based on the data set from Beck et al. (2018). Using zonal statistics, the climate zone that covers the relatively largest part of the area (that constitutes the majority of pixels) was attributed to each county/commune.

We attributed a Continentality Index value to each county/commune. The Continentality Index measures the annual range of temperature, this range increases over land in the lands farthest from the sea as a consequence of the different heat capacities of the seawater. In our calculations this index has been applied in its simplified form (Noce et al., 2020), this differs from the one developed by Driscoll and Yee Fong (1992) and is calculated as the difference (in °C) between the mean temperature of warmest and of the coldest months of the year. The Continentality Index here is based on the BioClimInd data set (Noce et al., 2020). Using zonal statistics, the mean of the continentality value within each area was attributed to each county/commune.

Degree of urbanization values were assigned to each county/commune and used as a statistical control in our analyses. "The degree of urbanization is the relationship between the population living in urban (and rural) areas and the total population of the municipality," based on the Global Human Settlement Layer (GHSL) (Pesaresi et al., 2019 [data]; Florczyk et al., 2019 [report]). The Global Human Settlement Layer (GHSL) is a refined version of the degree of urbanization (Eurostat, 2011; European Commission, 2021; Schiavina et al., 2019), where grid cells are classified after population size, population, and built-up area densities, based on satellite data (Corbane et al., 2017, 2019; Corbane, Florczyk, et al., 2018; Corbane, Politis, et al., 2018). The Global Human Settlement Layer (GHSL) classifies each pixel, excluding water, ranging from "very low density rural grid cell" to "urban center grid cell" (Florczyk et al., 2019). Using the degree of urbanization, even in large counties or municipalities with low population density, population accumulations are identified (cf. Dijkstra et al., 2020) and thereby, risk areas for COVID-19 spread. Using zonal statistics, the mean value for the degree of urbanization of the GHSL was attributed to the counties of Germany, Italy, and Spain, and the maximum value for the degree of urbanization was attributed to the communes of Norway and Sweden (see Figure S2 in Supporting

Information S1). The degree of urbanization for the five countries is thus not directly comparable for all five countries. The reason for this difference in expression is that urbanized areas in the huge northern municipalities of Norway and Sweden would be "swallowed" in the mean values, whereas a maximum value for Germany and Italy would "swallow" rural areas. For Spain, no expression worked ideally but the mean gave a better result. The aim of the degree of urbanization was to achieve intra-country differences that resulted in as many relative values as possible, to show in-country differences in the degree of urbanization. In all five countries, the capitals display high degrees of urbanization, but apart from that, the number and localities of urbanized areas varies (see Figure S2 in Supporting Information S1). As expected, there was a positive relationship between the degree of urbanization and COVID-19 incidence in all countries except Spain. The lack of a relationship between urbanization and COVID-19 in Spain is likely due to a restriction of range; Spain had only four relatively low values of urbanization (see Table S1 in Supporting Information S1). We normalized our data against the degree of urbanization by regressing urbanization on COVID-19 incidence and saving the residuals; the saved residuals represent incidence without urbanization bias (cf. Rader et al., 2020).

The resulting values of COVID-19 incidence, Köppen-Geiger climate zone, Continentality Index, and the degree of urbanization for the counties/communes for each county were exported from ArcGIS Pro in tabular format and statistically analyzed in SAS v9.4. To examine the relationship between COVID-19 incidence and climate zones and continentality across countries we created two residualized scores. For analyses completed separately by country, we adjusted for the degree of urbanization; for analyses completed across countries, we adjusted for both country and the degree of urbanization. We examined differences in residualized total incidence between climate zones using analysis of variance (ANOVA). The relationships between residualized total incidence and continentality were examined using linear regression, testing for both linear and quadratic relationships. As a secondary analysis, we conducted multivariate adaptive regression splines (MARS) modeling of the relationship between continentality and residualized total incidence to identify discontinuities, or knots, directly from the data (Bilenas & Herat, 2016).

Finally we used our statistical results to produce a COVID-19 probability map in GIS. We use the ranking of the climate zones and continentality that our results show from low to high COVID-19 incidence, and reclassify the values accordingly (see Table S3 in Supporting Information S1). These values were then added in the raster calculator in ArcGIS Pro to show a combined probability map (cf. Ebert et al., 2016).

3. Results

3.1. Spatial Analysis

3.1.1. Spatial Pattern of COVID-19 Total Incidence

The mapped total incidence for the five countries from March 2020 to mid-July 2021 shows a patchy pattern (Figure 1). An observable pattern shows relatively lower incidence values in the west of countries with an open western coastline toward the Atlantic Ocean: the entire coast of Norway, north-west Germany, and north-west Spain. This also goes for the Italian islands with an open western coastline in the Mediterranean. The only country lacking an open western coastline and the associated pattern is Sweden. Relatively high incidences can be found in all five countries in the counties/communes that hold the capital cities. However, these are not necessarily the areas with highest incidences.

The highest incidences for Norway are found in the south-east of the country, in the area of the capital also in the surrounding communes. Two single outliers with high incidences in the south of the country, and one in the very north break the pattern of otherwise generally low incidence values.

Sweden shows a rather patchy pattern with highest incidence in the southern highlands, along the northern half of the East-Coast toward the Baltic, and in some communes in the northern half of the country.

The highest incidence values in Germany are distributed along the south-eastern border of the country, with the absolutely highest values in Saxony at the border to Czechia. Single outliers with higher values exist in the south-west and in the north-west. Generally Germany shows a pattern of incidences from low to high in a north-west to south-east direction.

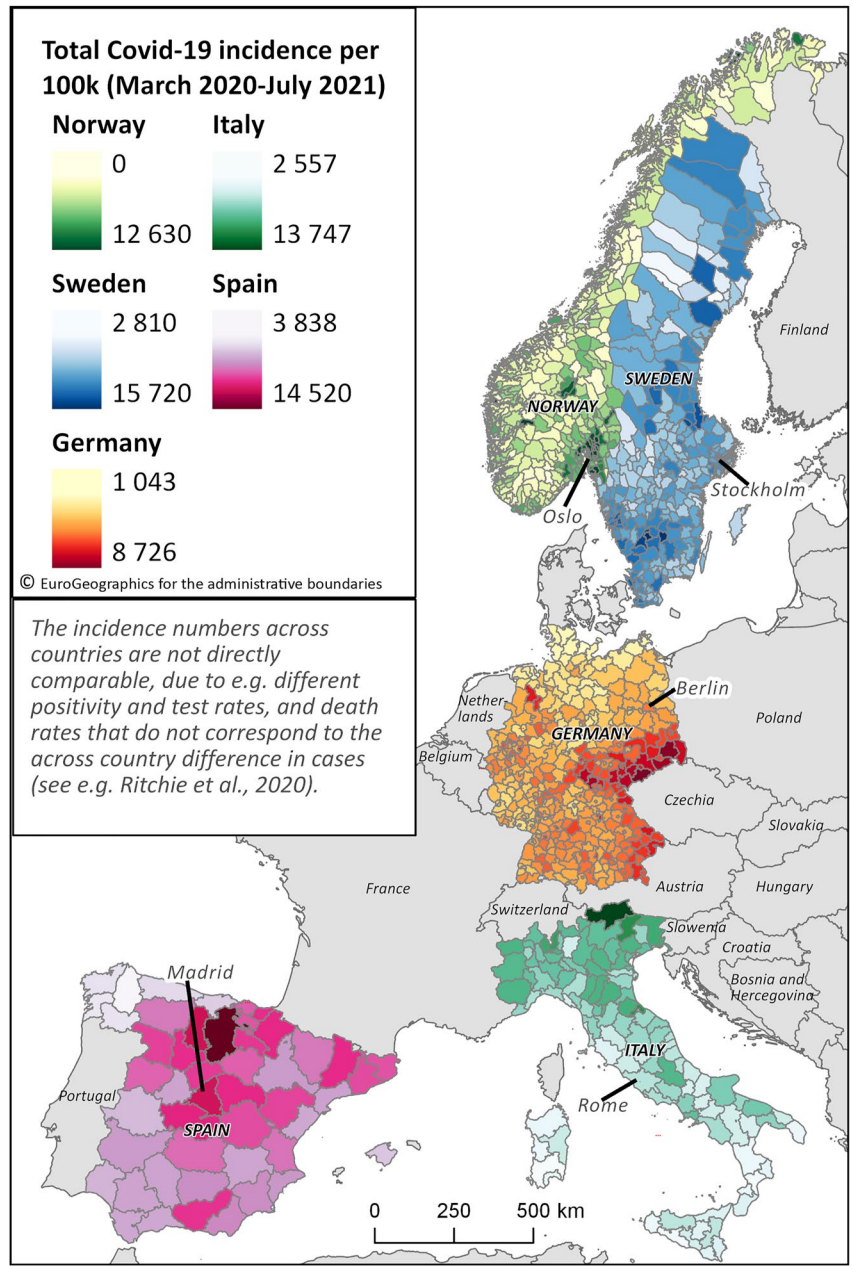

Figure 1. Total (cumulated) incidence of reported SARS-CoV-2 occurrence per 100,000 inhabitants for the five countries from the reports between March 2020 and mid-July 2021. Based on data from the Norwegian Institute of Public Health (Folkhelseinstituttet), incidence calculated in VG (2021); the Public Health Agency of Sweden (FHM, 2020), the Robert-Koch Institute, Germany (Robert Koch Institut, 2020); the Italian Ministry of Health (Ministero della Salute) (Github, 2021) (Italy) and CNECovid (2021) (Spain). The total incidence in this article is treated as a *relative value*. The relation between the reported cases, the death rate and the conducted tests differs spatially and temporally within and across countries and makes a meaningful country-to-country comparison of the total incidence challenging (cf. data for death rates, tests, etc. on https://ourworldindata.org/coronavirus).

In Italy the highest incidence values are concentrated in the north of the country at the border to or in the Alps, and along the Mediterranean east-coast, with one outlier with higher values in the central Italian mountains (Apennines).

The highest incidence in Spain is found in the northern half of the country, at the border to Spain, and in the capital county. However, the low to high south to north pattern shows an exception in the northwestern corner of

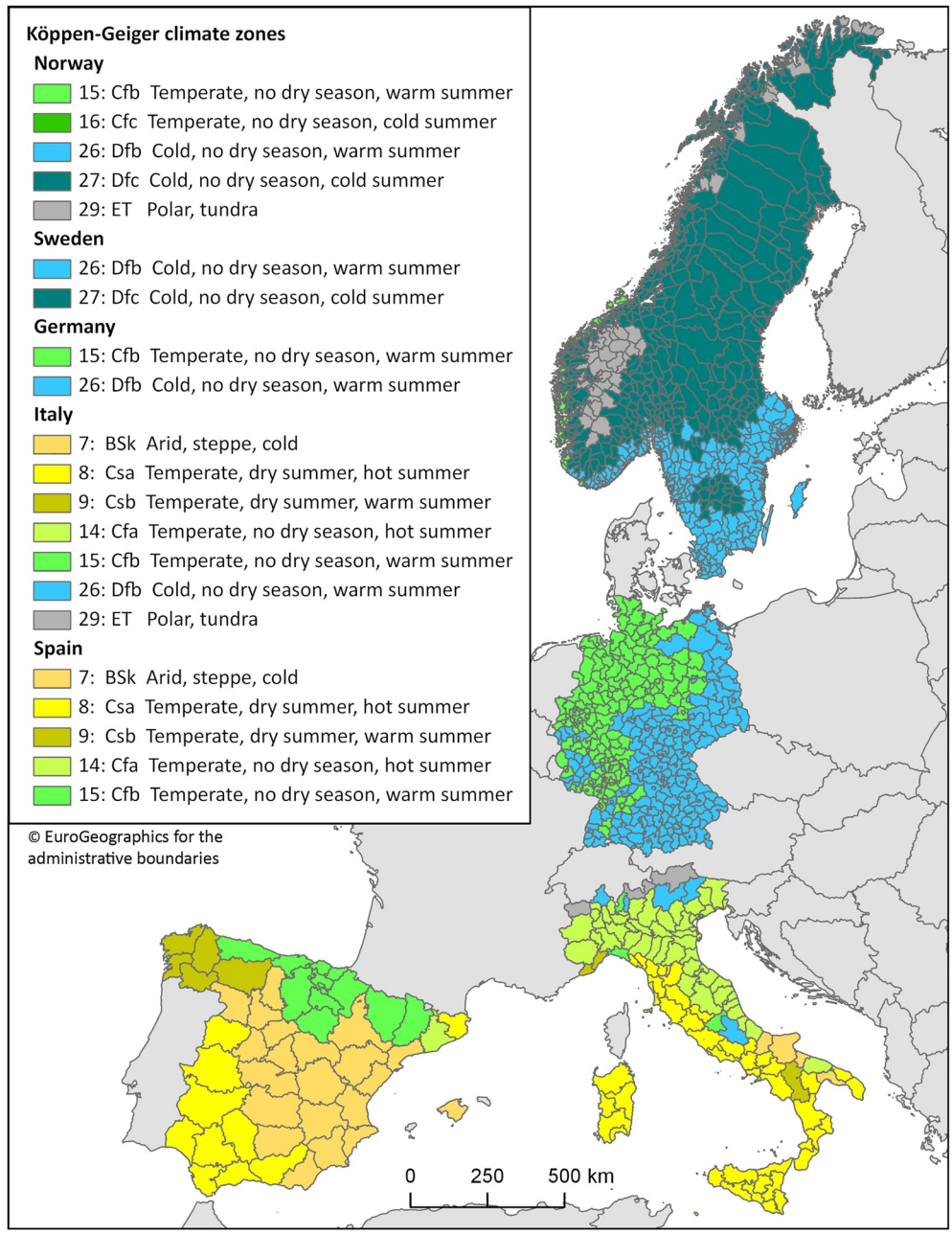

Figure 2. Köppen-Geiger climate zones for the largest part of the area per municipality (Norway, Sweden) or county (Germany, Italy, Spain). Based on Beck et al. (2018).

the country, in six counties with a western coastline to or close to the Atlantic. These six counties clearly show the lowest incidence values for Spain.

3.1.2. Spatial Pattern of Köppen-Geiger Climate Zones

The Köppen-Geiger climate zones are defined by a classification based on a combination of temperature and precipitation range. The countries we investigate comprise nine Köppen-Geiger climate zones (Figure 2). The vast majority of Norway, with the exception of the south-west coast in a temperate climate, is located in cold climate zones. Some of the highest ranges of the northern Scandes mountain chain, and northernmost areas, hold a Polar climate. Sweden is entirely located in two cold climate zones. The northwestern part of Germany is located in temperate climate, the southeastern part in a cold climate zone. Italy has the widest range of climate

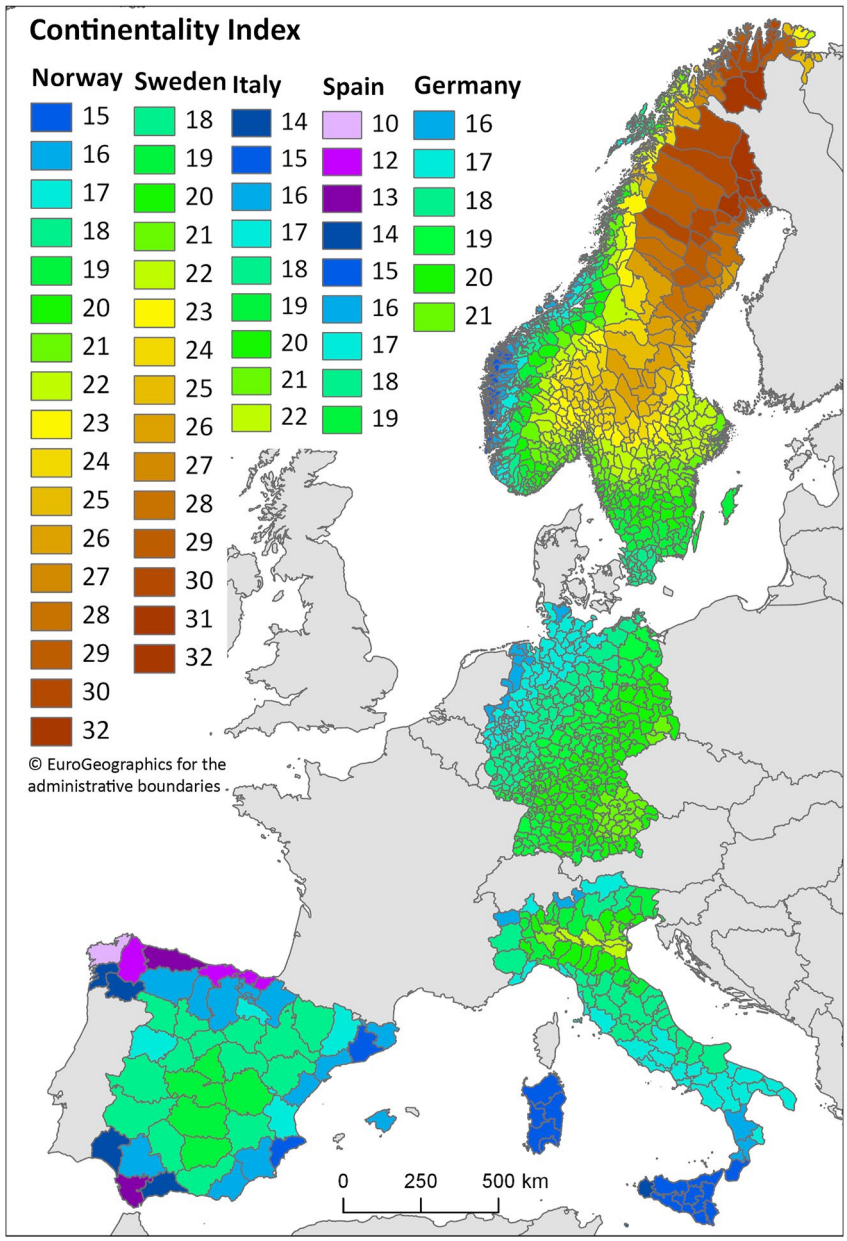

Figure 3. Mean Continentality Index per municipality (Norway and Sweden) or county (Germany, Italy, and Spain). Continentality Index raster data from Noce et al. (2020).

zones (7), however, only few counties are located within the cold and polar climate zones (in the Alps and on the highest elevations of the central Apennines). The majority of the country is located in temperate climates, and some counties on the southern part of the east coast in an arid climate. This arid climate zone comprises the majority of Spain in the central-eastern zone. The rest of Spain, along the northern and western boundaries, has temperate climates.

3.1.3. Spatial Pattern of the Continentality Index

The five countries we investigate have all different ranges of continentality (Figure 3), where north-west Spain reaches the lowest level of continentality (the highest level of oceanicity) with the value of 10 and northern Norway and Sweden the highest continentality, with the value of 32.

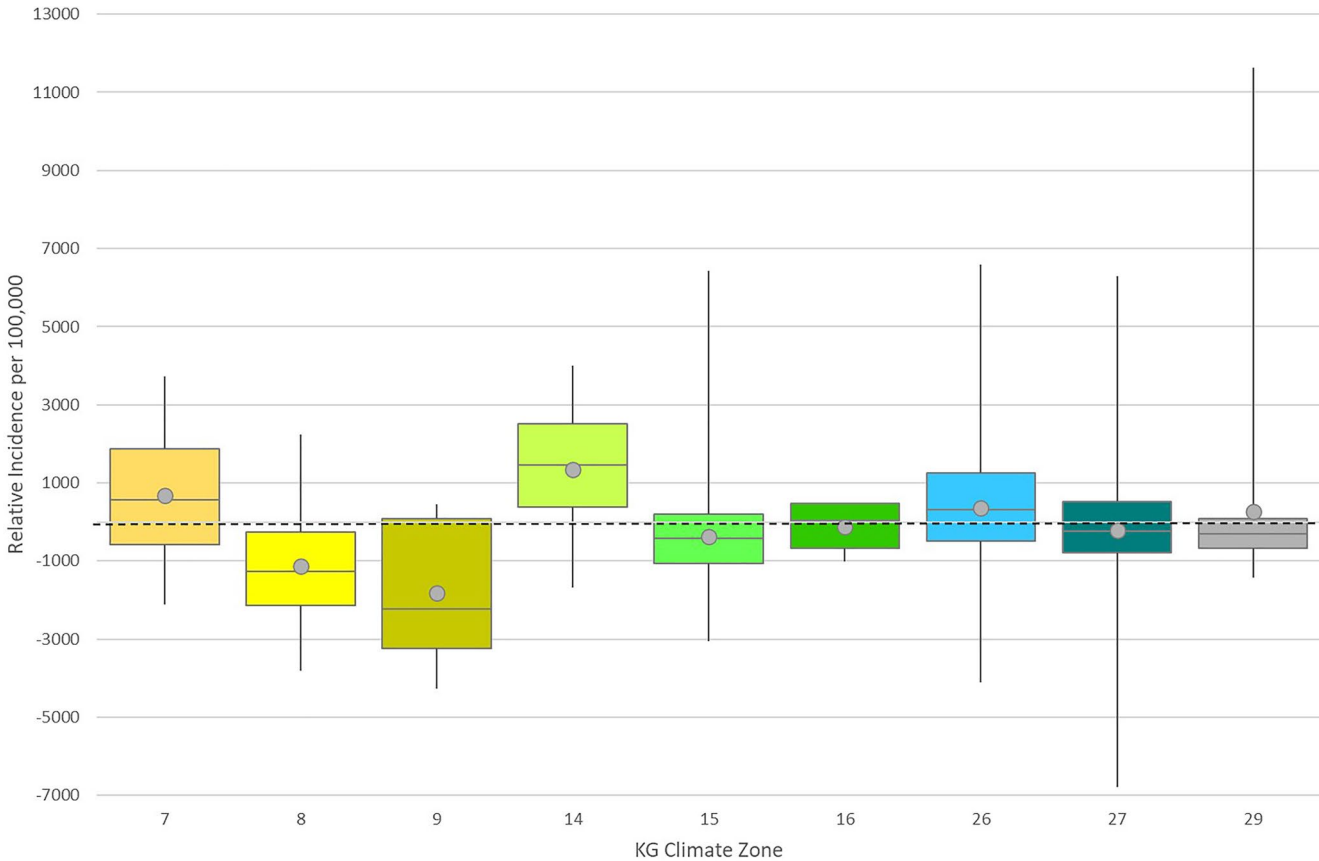

Figure 4. The relative distributions for each KG climate zone after regressing out the degree of urbanization and mean-level differences between countries in overall incidence rates. Boxes represent the interquartile range (Q1 to Q3), the middle line in each box represents the median value, circles represent the mean, and whiskers represent the minimum and maximum values for each KG climate zone.

However, Norway has the widest range of values, with a rather low continentality (15) at its southwestern coast line, and higher ranges of continentality, above a value of 25, are only reached on the northernmost peninsulas of the country. In contrast, Sweden reaches a high continentality much further south and almost the entire northern half of the country displays continentality values of 27 and higher. This makes Sweden by far the most continental country of the five. Germany has the lowest range of values, from 16 to 21, with the lowest continentality at the north-western coast and increasing values across the country in a north-west to south-east direction. Italy has a slightly larger range of values than Germany, with low values of 14 and 15 on the western islands and a lowest value of 22 in northern central Italy. Spain, with the lowest value of 10 in the north-west, low values of 10–16 along its entire coastline, and the highest values of up to 19 in the center of the country, is the most maritime country in range.

3.2. Mean Differences in Total COVID-19 Incidence by Köppen-Geiger Climate Zones

If we statistically adjust for country differences in incidence, and control for the degree of urbanization, the KG climate zones formed four distinct groups. Climate zones KG8 and KG9 had significantly lower total incidence than other climate zones. Climate zones KG15, KG16, and KG27 formed the next group; KG29, KG26, and KG7 formed the next group with even higher incidences; and climate zone 14 had significantly higher total incidence than any other climate zone (Figure 4; Table 1).

Climates with larger annual differences in temperature and rainfall distributed throughout the year (temperate climate zone 14, cold climate zones 26, and cold arid 7 and polar 29) have a higher total COVID-19 incidence than climate zones with smaller annual differences in temperature and dry summers and winter rain (=unevenly

Table 1
Köppen-Geiger Climate Zones and Their Temperature and Precipitation Properties, Sorted Into Four Groups From Highest to Lowest Total COVID-19 Incidence in the Five European Countries, When Controlled for the Degree of Urbanization, and After Regressing Out Mean-Level Differences Between Countries in Overall Incidence Rate (Climate Zone Criteria Modified From Beck et al. (2018) and Forkel (2015))

Total Incidence	Köppen-Geiger climate zone
Highest	**14 Cfa – Temperate, no dry season, hot summer**. Temperature of warmest month 22 °C or higher, temperature coldest month less than 18 °C but more than 0 °C. The driest month has more than 3 cm of precipitation.
	7 BSk – Arid, steppe, cold. Average annual temperature less than 18 °C. Little precipitation all year.
	26 Dfb – Cold, no dry season, warm summer. Temperature warmest month 10 °C or higher and lower than 22 °C, temp of coldest month 0 °C or lower. Number of months with air temperature more than 10 °C 4 or higher. Precipitation all year.
	29 ET – Polar, tundra. Temp of warmest month less than 10 °C but more than 0 °C. Precipitation all year.
	16 Cfc - Temperate, no dry season, warm summer. Temperature warmest month more than more than 10°C but less than 22°or higher, temperature coldest month less than 18 °C but more than 0 °C. Number of months with air temperature more than 10 °C 1 or more but less than 4. Precipitation all year.
	27 Dfc – Cold, no dry season, cold summer. Temperature warmest month 10 °C or higher and lower than 22 °C, temp of coldest month 0 °C or lower and more than -38 °C. Number of months with air temperature more than 10 °C, but less than 4 °C. Precipitation all year.
	15 Cfb – Temperate, no dry season, warm summer. Temperature of warmest month 10 °C or higher, temperature of coldest month less than 18 °C but more than 0 °C. Number of months with air temperature more than 10 °C 4 or higher, but warmest month less than 22 °C. Precipitation all year.
Lowest	**8 Csa - Temperate, dry summer, hot summer**. Temperature warmest month more than 10 °C, temperature coldest month less than 18 °C. Temperature of warmest month more than 22 °C. Precipitation of driest summer month less than 3 cm and less than a third of precipitation of wettest winter month.
	9 Csb – Temperate, dry summer, warm summer. Temperature warmest month more than 10 °C, but less than 22 °C. Temperature coldest month less than 18 °C. Number of months with air temperature more than 10 °C 4 or higher. Precipitation of driest summer month less than 3 cm and less than a third of precipitation of wettest winter month.

distributed annual precipitation) (temperate climate zones 8 and 9). Consequently, climate zones with lowest incidence values in our study area are climate zones with a clear divide of dry and wet seasons.

3.3. Relationship Between Total COVID-19 Incidence and the Continentality Index

We first ran linear and quadratic regression models with the degree of urbanization-adjusted total incidence as the dependent variable and continentality as the independent variable, separately by country (Figure 5). Linear models explained between 0.3% (Norway) and 30.8% (Italy) of the variance in total incidence (see Table S2 in Supporting Information S1). In all countries except Norway and Sweden, the linear trend was significantly positive. For Norway, the linear slope was not significantly different from zero; for Sweden it was significantly negative. Quadratic models explained between 0.8% (Norway) and 36% (Italy) of the variance.

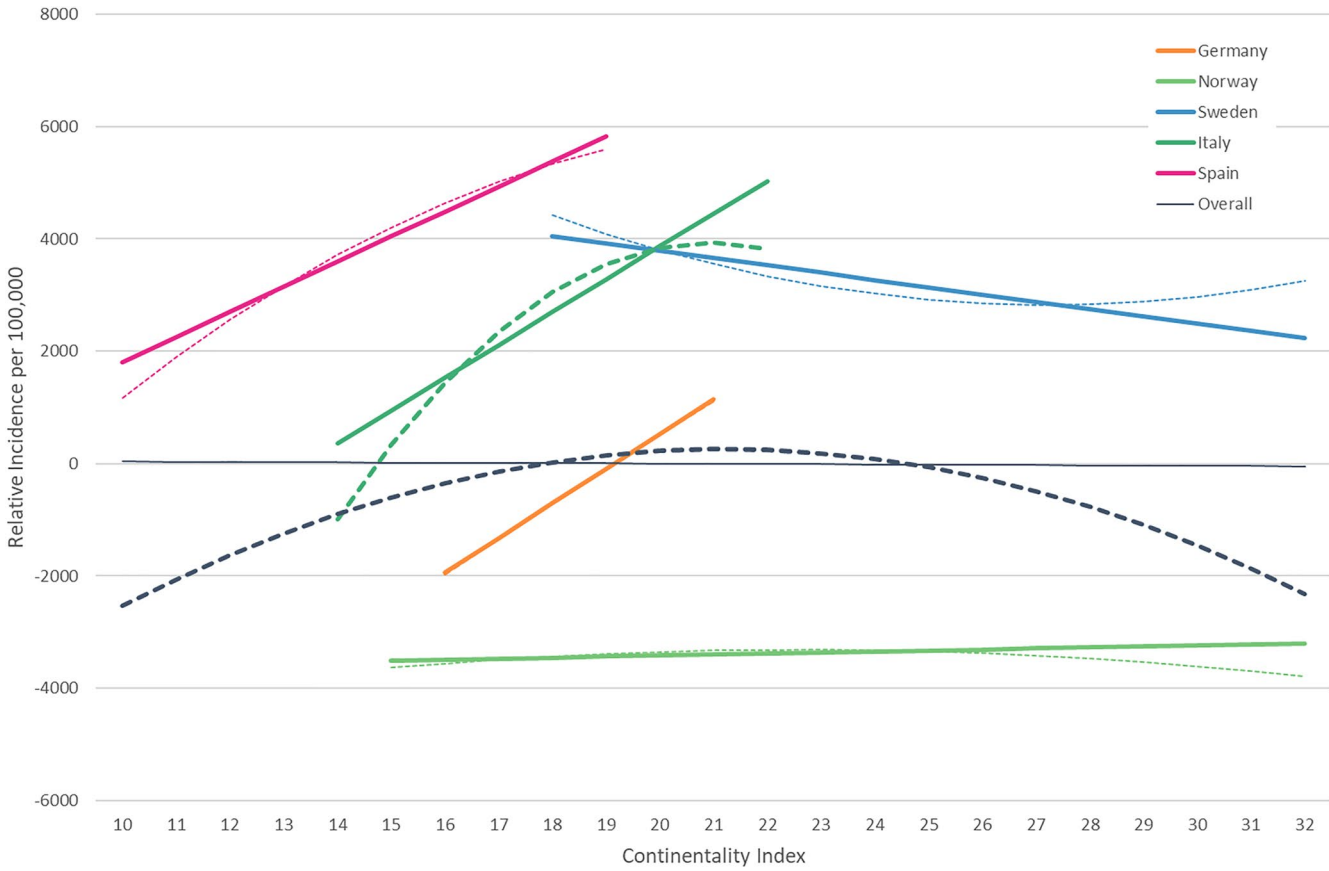

Figure 5. The figure graphs, the predicted linear, and quadratic relationships between the Continentality Index and residualized total incidence (residualized for the degree of urbanization for country-specific analyses; residualized for country and the degree of urbanization for overall analyses). Lines for each country only include the Continentality Index values observed in that country. Thinner lines indicate that the linear trend for Norway and overall multicountry linear trend between total incidence and continentality was not statistically significantly different from zero and that the quadratic trends between total incidence and continentality for Germany, Norway, Sweden, and Spain were not statistically significantly different from zero. Model results are presented in Table S2 in Supporting Information S1.

The quadratic term did not add significantly to the explanation of total incidence in four countries (Germany, Norway, Sweden, and Spain). It did add significantly to the explanation in Italy, which saw rising total incidence at lower values of the Continentality Index and declining total incidence at higher values of the Continentality Index. Figure 5 graphs the predicted linear and quadratic relationship for each country, including only those continentality indices that were observed in the country.

To examine the effect of the full range of continentality indices on total incidence, we ran linear and quadratic regression models with country- and the degree of urbanization-adjusted total incidence as the dependent variable and continentality as the independent variable. The linear model accounted for <0.1% of the variance in adjusted total incidence and continentality showed no significant linear relationship with adjusted total incidence. The quadratic model accounted for 5.2% of the variance in adjusted total incidence. Continentality showed a significant linear trend with each 1-unit change in continentality adding 98 more cases to the adjusted total incidence. There was also a significantly negative quadratic trend, such that adjusted total incidence rose through approximately a Continentality Index of 19–23, at which time total incidence began to decline.

To further examine the nonlinear relationship between adjusted total incidence and continentality, we conducted a follow-up analysis using multivariate adaptive regression splines (MARS) modeling. multivariate adaptive regression splines (MARS) is a flexible, nonparametric regression technique used to identify discontinuities, or knots, directly from the data (Bilenas and Herat, 2016); in our case, it is purely exploratory and results will need to be replicated in other samples. We used a random draw of 50% of our sample for training, 25% for testing, and

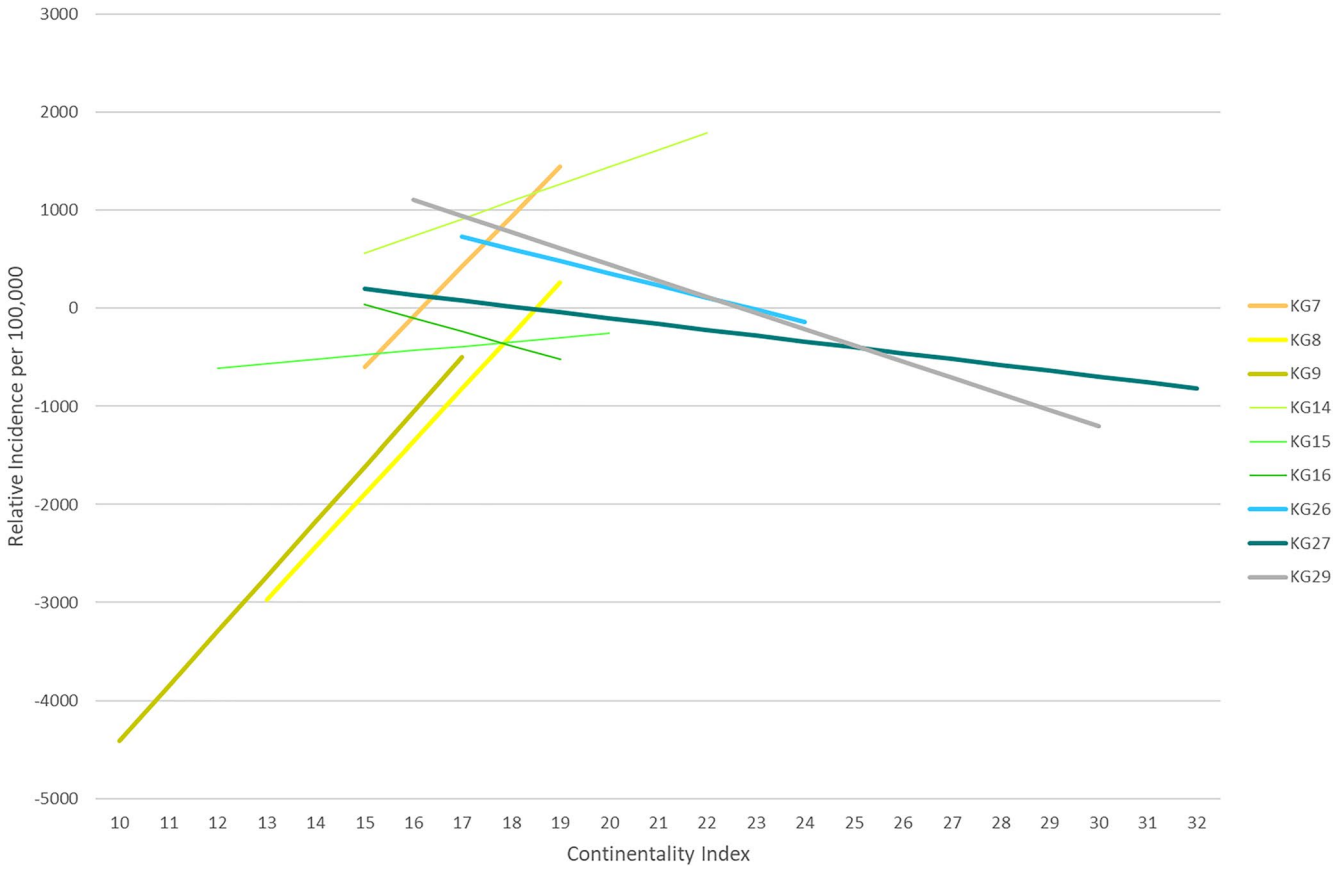

Figure 6. The figure graphs the predicted linear relationships between the Continentality Index and residualized total incidence (residualized for country and the degree of urbanization). Lines for each climate zone only include the Continentality Index values observed in that climate zone. Thinner lines indicate that the linear trends for KG's 14, 15, and 16 were not statistically significantly different from zero.

25% for validation. Results indicate two significant discontinuities in the relationship between residualized total incidence and continentality at 19 and 24, such that the relationship between total incidence and continentality is positive before 19, negative between 19 and 24 and not significantly different from 0 thereafter.

3.4. Relationship Between COVID-19 Incidence and Continentality in Different Köppen-Geiger Climate Zones

In Köppen Geiger climate zones 7, 8, and 9 there was a significantly positive linear relationship between continentality and total country-adjusted incidence, such that each 1-unit change in continentality adds ∼500–560 to the total incidence per 100 K. In Köppen Geiger climate zones 14, 15, and 16 there was no significant linear relationship between continentality and total country-adjusted incidence. In Köppen Geiger climate zones 26, 27, and 29, there was a significantly negative linear relationship between continentality and total country-adjusted incidence such that each 1-unit change in continentality decreases total incidence by ∼120 per 100 K (Figure 6).

3.5. Pattern of COVID-19 Spread Probability Based on Continentality and Climate Zone

We translated our statistical results to a visual GIS-map (Figure 7) that shows the probable pattern of COVID-19 spread in the five countries that comprise our study area, if continentality and climate zone were the exclusive determining parameters. We ranked the climate zones and continentality accordingly to produce the probability map (see reclassification values for the ranking in Supporting Information S1). The map is purely based on our results, showing the probability after residualizing across country differences and the degree of urbanization.

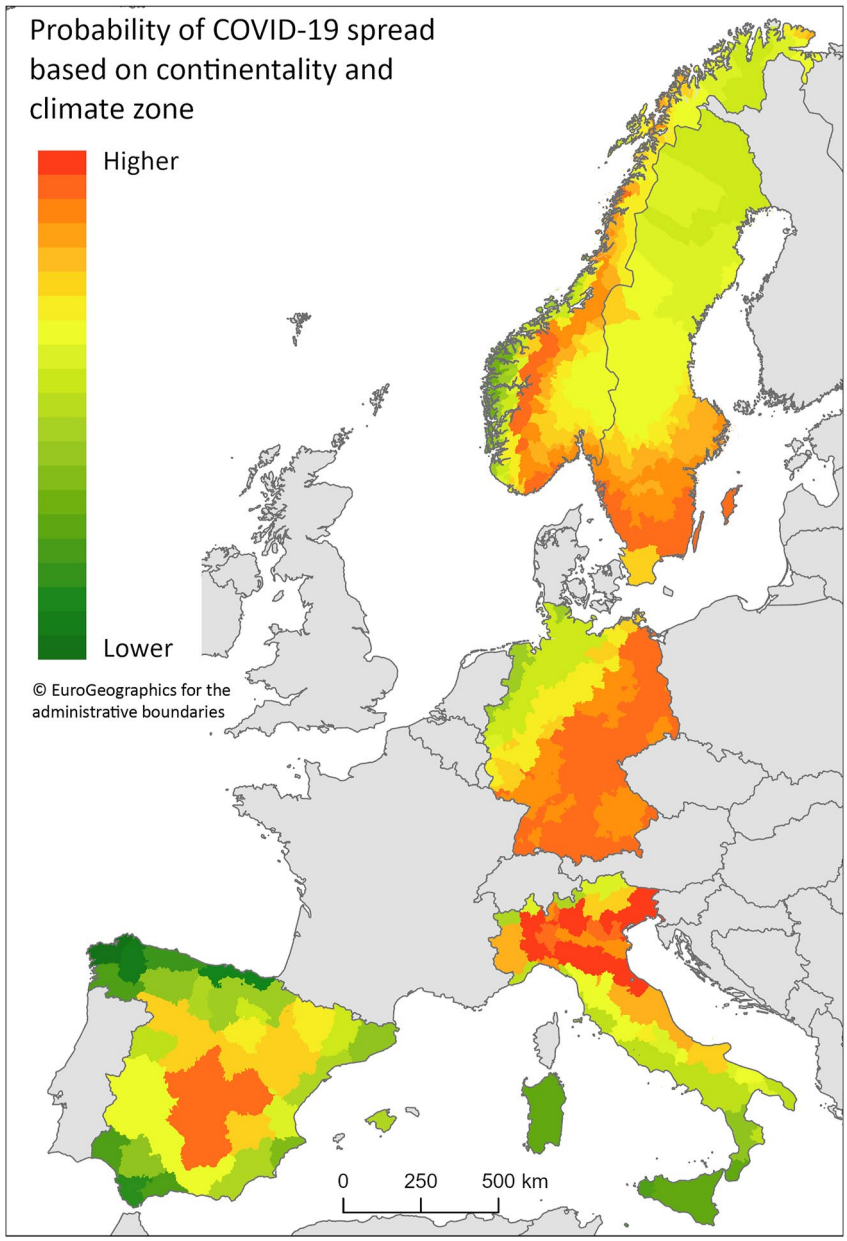

Figure 7. The probability for the spread of COVID-19, weighed after the statistical results of this paper, for the influence of continentality and climate zones. Thereby, other possible influencing parameters such as the degree of urbanization are excluded.

4. Discussion

After controlling for the degree of urbanization and cross-country differences, the ranking of climate zones results in four groups with different COVID-19 incidences. The highest incidence is within climate zone 14—Temperate, no dry season, hot summer. Within the temperate (mild) climates represented in the five countries studied, this is the temperate climate with the highest differences in temperature. Like the other climate types we find with higher incidence numbers, this climate type has no clear dry or wet season, rather precipitation occurs throughout the year. Climate zone 14 is not well represented in Europe; in the five countries of our study it comprises the north of Italy and one county in north-east Spain. As for northern Italy, this area is rather special from a topographic point of view as it is surrounded in the west and the north by the Alps, which shields it from the influence of the west-wind zone and by that from oceanic influence (further explained in the next section about

the Continentality Index). Köppen-Geiger climate zones are defined by values of temperature and precipitation. Minimum temperatures have been found to correlate with COVID-19 propagation, where lower temperatures promote COVID-19 spread (Loché Fernández-Ahúja & Fernández Martínez, 2021). Our findings are similar in that the group of climate zones with the lower mean and minimum temperatures have higher total incidence. Additionally, the two temperate winter-rain climate zones with highest mean temperatures (8 and 9) had the lowest total incidence. The climate zone with the highest total incidence is nonetheless not the climate zone with lowest mean temperatures. This might not be necessarily contradictory, as Köppen-Geiger climate zones are a summary of climate indicators, and correlations of COVID-19 and temperature would need a temporal resolution.

In our data we find a peak of cumulated COVID-19 incidence at Continentality Index values 19–24, rising steep from lower values to 19, slowly falling until 24, and thereafter barely falling at all (statistically no different from zero). Possible reasons for a decrease in cases above 19 might be lower populations in areas with rising continentality indices among our study countries. This is the case for Norway and Sweden, where the Continentality Index is rising toward the northern inland with harsher living conditions. However, Italy also shows incidences falling in areas with a Continentality Index of 20 and above; this happens in one of the areas with the highest degrees of urbanization, the Venice area of northern Italy. Seen in a wider context, countries in Europe that fall entirely within continentality indices 19–21, like Czechia, Bosnia, and Herzegovina, Northern Macedonia and Montenegro, display the highest accumulated COVID-19 death rates in Europe, where countries further east with continentality indices above 20, like Poland, Finland, Lithuania, Slovakia, and Ukraine, have lower death rates at the date of writing in November 2021 (cf. Ritchie et al., 2020, Our World of data, for death rates).

It is worth unpacking what makes the Continentality Index range of 19–24 a favorable value for high COVID-19 infection rates. Either, this value is a proxy for another phenomenon, or the value itself, that is, the range of temperature has a direct effect. The continentality displays the influence of the ocean, a function of distance and topographical hinders and the dominating wind direction. Europe falls in the west-wind zone of the northern hemisphere, the so-called westerlies. The Continentality Index is lowest at open west coast areas such as north-eastern Spain and is (irregularly) rising toward the east. This is also the case for the USA, the other great landmass in the westerlies. Torregrosa et al. (2013) described continentality categories for the wider San Francisco area on the US west coast. If we would apply these values to our study area, Continentality Index values up to 17 fall in an oceanic category, values of 17–21 are described as semicontinental, and values >21 as subcontinental. By this, the values where we find the highest COVID-19 incidence would fall right outside the oceanic influence and into the category "semicontinental." This suggests that maritime climates may suppress COVID-19 infectiousness, and confirms the results of earlier studies that found mild and humid coastal climates limit COVID-19 contamination (e.g., Piazzola et al., 2021). However, the question as to why cases are falling in subcontinental conditions remains for the moment unsolved.

Studies in the early stages or about the early stages of the COVID-19 pandemic have shown contradictory or inconsistent relationships between climate factors and the spread of the virus (e.g., Sera et al., 2021). These studies commonly only include one climate factor, such as temperature, and not climate systems. Also, they only include the first wave of the pandemic. First waves of pandemics behave erroneously, as they hit a population with a completely unprepared immune system and only in later waves, does a seasonal pattern of infection emerge (Chandra et al., 2020). But even in later studies, certain temperatures and air humidity have been shown to be inconsistent with the virus spread (Choi et al., 2021). Alternative environmental factors that showed more correlation than temperature and humidity were air drying capacity and ultraviolet radiation (Choi et al., 2021). However, the main argument why air drying capacity might be a factor was the transport of droplets, which then was still the presumed spreading mechanism for COVID-19, was later corrected, as COVID-19 also spreads with aerosols (Chen, Jia, Han, 2021; Chen, Prettner, et al., 2021). Ultraviolet radiation has been in discussion as a driver for respiratory virus seasonality for decades, however, never with entirely conclusive results (Jensen, 1964); when investigated for the Sars-Cov-2, Sagripanti and Lytle (2020) showed a probability of inactivation of the virus during summers in higher ultraviolet radiation in Italy. Most of these factors show a better correlation with the seasonality of respiratory viruses in the northern hemisphere and get illusive in the tropical/equatorial zone (cf. Bloom-Feshbach et al., 2013).

We look at the total incidence and not directly seasonal difference in COVID-19 spread; however, in all five countries—entire Europe—the COVID pattern shows a clear seasonality. Lower total incidence means that the seasonal ups are weaker and/or shorter than in regions with higher total incidence. This means there is an indirect

connection to seasonality to climate zones and the Continentality Index. Martinez (2018) suggested a possible host susceptibility, meaning that environmental factors influence the host and not the virus. This would imply a host seasonality (Martinez, 2018) that in turn might be influenced by the distance to the ocean.

Death rates or ICU numbers might have been more comparable; however, only the incidence was available for the smaller special entities across all five countries. Incidence cannot be directly compared across countries, due to different testing numbers and other factors. However, a relative relation can be given. We residualize against country differences to find the overall correlation with continentality and climate zones. The incidence varies across and within countries. The discussed possible reasons for this variety are manifold, such as vaccination rate, the possibility and willingness to distance keeping, social factors, access to healthcare and others (Bendavid et al., 2021; Brauner et al., 2021; Choi et al., 2021; Haas et al., 2021; Loomba et al., 2021; Prata et al., 2021), and socio-economic factors (Buja et al., 2020; Ehlert, 2021). We look at the overall main pattern that shows a lot of "noise" because of these factors.

At the current date (November 2021) the low to high incidence patterns within the five countries as described in our paper are persisting or even manifesting. By now between 65% and 90% of the population in the five countries we investigate are vaccinated and the majority of COVID-19 patients in ICU and death are unvaccinated (cf. Robert Koch Institut). The pattern of low to high persists nonetheless, and the time span of our investigation only includes the very first months of vaccination, with around 30% of the population vaccinated at the end of our time span in the overall low-incidence summer time (Ritchie et al., 2020). We thereby assess vaccinations not to impact our results.

Our study has limitations. First, the pandemic occurred through time with different surges at different times in different countries. Our analysis does not take this time variation into account; since this was the first look at the effect of climate zones and continentality on COVID-19 incidence we wanted to first establish an overall relationship before examining timing effects. Future studies will need to take this time variation into account to more fully explore which climatological parameters have the most effect on COVID-19 incidence. Second, our study was limited to five countries in Western Europe. Concentrating on the west-wind zone of Europe limited the potential range of Köppen Geiger climate zones we could study and may limit generalizability beyond Europe. We chose these countries because they provided easy access to municipality and county level COVID-19 data. Future studies should attempt to replicate our findings in a broader sample of countries representing different continents and a wider range of climate zones. Third, there are multiple other social vulnerability measures beyond urbanization that we could have statistically controlled for (cf. Islam et al., 2021). For example, population density has been widely investigated, with diverging results (Paez, 2021); we chose urbanization to normalize our data because high urbanization has been shown to better explain high COVID-19 incidence than population density (González-Val & Sanz-Gracia, 2021). Fourth, social vulnerability and mitigation measures may have a considerable influence on incidence (Kashem et al., 2021); particularly at the beginning of the pandemic, these measures were inconsistently applied across Europe and not well documented or easily obtained. Our analyses attempted to take these potential country-level differences into account by adjusting for mean level differences in COVID-19 incidence when examining cross-country effects. Finally, our study considers two main climate indices (Köppen Geiger climate zones and the Continentality Index). As previously mentioned they describe long-term average climatic conditions and do not allow us to identify short-term phenomena (related to meteorology) that may locally increase or decrease the risks to human health.

5. Conclusions

According to our results for Norway, Sweden, Germany, Italy, and Spain, during the first period of the COVID-19 pandemic from March 2020 to July 2021, climates with larger annual differences in temperature and precipitation all year (temperate climate zone 14, cold climate zones 26, and cold arid 7 and polar 29) have higher total COVID-19 incidence than climate zones with smaller annual differences in temperature and dry summers and winter rain (=unevenly distributed annual precipitation) (temperate climate zones 8 and 9).

Maritimity has a strong suppressing effect on total COVID-19 incidence. Up to a Continentality Index of 19, the total incidence in the study area rose steeply. Starting from 19 to 24, it slowly fell, thereafter, it fell slightly, but the decline was not statistically significantly different from zero. The total Covid-19 incidence was lowest at

open west coast areas, which have the lowest Continentality Index values and are in temperate climate zones 15, 8, and 9. Taken together, the "best climatic conditions" to forestall COVID-19 spread in our study of countries in the European west-wind zone would be all areas with an open west coast (i.e., north-western Spain, the Italian islands, the German north-sea coast area, and the south-western coast of Norway). Although Sweden's lowest Continentality Index values are observed at its southern coastal area, the value of 18 is still relatively high and not in a favorable climate zone. From this perspective, Sweden does not have a clear "best climatic condition" area.

The "worst climatic conditions" for forestalling COVID-19 spread in the countries studied would be the Oslo area and the south-eastern coast stretch of Norway, southern central Sweden, and the west-east area bordering to that, including Göteborg and Stockholm, south-eastern Germany including Saxony and Bavaria, northern central Italy including Lombardia, and central Spain, including Madrid. Healthcare decision makers in these area should expect greater COVID-19 spread.

Conflict of Interest

The authors declare no conflicts of interest relevant to this study.

Data Availability Statement

COVID-19 incidence data for the different countries are available from the websites given with links in the references, guided by the ministry of health (or corresponding) in each country. Continentality Index data from Noce et al. (2019) used in this study can be freely downloaded from Pangaea repository (https://doi.pangaea.de/10.1594/PANGAEA.904278) and from CMCC Foundation Data Delivery System (https://dds.cmcc.it/#/dataset/bioclimind/historical) Köppen-Geiger data from Beck et al. (2018) can be downloaded at http://www.gloh2o.org/koppen/. The degree of urbanization (Global Human Settlement Layer, GHSL), Pesaresi et al. (2019) is available on https://publications.jrc.ec.europa.eu/repository/handle/JRC117104. County and commune borders for Norway, Sweden, Germany, Spain and Italy from Eurostat (2020) are available from https://ec.europa.eu/eurostat/web/gisco/geodata/reference-data/administrative-units-statistical-units/. Our data sets for GIS and statistics are available on Ebert et al. (2022), https://doi.org/10.5281/zenodo.5900811.

Acknowledgments
The authors thank two anonymous reviewers for their thoughtful comments that helped to improve the manuscript.

References

Ahasan, R., & Hossain, M. M. (2021). Leveraging GIS and spatial analysis for informed decision-making in COVID-19 pandemic. *Health Policy and Technology*, *10*(1), 7–9. https://doi.org/10.1016/j.hlpt.2020.11.009

Al-Kindi, K. M., Alkharusi, A., Alshukaili, D., Al Nasiri, N., Al-Awadhi, T., Charabi, Y., & El Kenawy, A. M. (2020). Spatiotemporal Assessment of COVID-19 spread over Oman using GIS techniques. *Earth Systems and Environment*, *4*, 797–811. https://doi.org/10.1007/s41748-020-00194-2

Bashir, M. F., Ma, B., Komal, B., Bashir, M. A., Tan, D., & Bashir, M. (2020). Correlation between climate indicators and COVID-19 pandemic in New York, USA. *The Science of the Total Environment*, *728*, 138835. https://doi.org/10.1016/j.scitotenv.2020.138835

Beck, H. E., Zimmermann, N. E., McVicar, T. R., Vergopolan, N., Berg, A., & Wood, E. F. (2018). Present and future Köppen-Geiger climate classification maps at 1-km resolution. , *5*(1), 180214. [Dataset] https://doi.org/10.1038/sdata.2018.214

Ben-Ahmed, K., Aoun, K., Jeddi, F., Ghrab, J., El-Aroudi, M. A., & Bouratbine, A. (2009). Visceral leishmaniasis in Tunisia: Spatial distribution and association with climatic factors. *The American Journal of Tropical Medicine and Hygiene*, *81*(1), 40–45. https://doi.org/10.4269/ajtmh.81.1.40

Bendavid, E., Oh, C., Bhattacharya, J., & Ioannidis, J. P. A. (2021). Assessing mandatory stay-at-home and business closure effects on the spread of COVID-19. *European Journal of Clinical Investigation*, *51*(4). https://doi.org/10.1111/eci.13484

Bilenas, J. V., & Herat, N. (2016). *Using Regression Splines in SAS® STAT Procedures*. SAS-Users Group. Paper BF-140. Retrieved from https://www.lexjansen.com/sesug/2016/BF-140_Final_PDF.pdf

Bloom-Feshbach, K., Alonso, W. J., Charu, V., Tamerius, J., Simonsen, L., Miller, M. A., & Viboud, C. (2013). Latitudinal variations in seasonal activity of influenza and respiratory syncytial virus (RSV): A global comparative review. *PLoS One*, *8*(2), e54445. https://doi.org/10.1371/journal.pone.0054445

Brauner, J. M., Mindermann, S., Sharma, M., Johnston, D., Salvatier, J., Gavenčiak, T., et al. (2021). Inferring the effectiveness of government interventions against COVID-19. *Science*, *371*(6531), eabd9338. https://doi.org/10.1126/science.abd9338

Buja, A., Paganini, M., Cocchio, S., Scioni, M., Rebba, V., & Baldo, V. (2020). Demographic and socio-economic factors, and healthcare resource indicators associated with the rapid spread of COVID-19 in Northern Italy: An ecological study. *PLoS One*, *15*(12), e0244535. https://doi.org/10.1371/journal.pone.0244535

Bull, G. (1980). The weather and deaths from pneumonia. *The Lancet*, *315*(8183), 1405–1408. https://doi.org/10.1016/s0140-6736(80)92666-5

Byun, W. S., Heo, S. W., Jo, G., Kim, J. W., Kim, S., Lee, S., et al. (2021). Is coronavirus disease (COVID-19) seasonal? A critical analysis of empirical and epidemiological studies at global and local scales. *Environmental Research*, *196*, 110972. https://doi.org/10.1016/j.envres.2021.110972

Chandra, S., Christensen, J., & Likhtman, S. (2020). Connectivity and seasonality: The 1918 influenza and COVID-19 pandemics in global perspective. *Journal of Global History*, *15*(3), 408–420. https://doi.org/10.1017/s1740022820000261

Chen, B., Jia, P., & Han, J. (2021). Role of indoor aerosols for COVID-19 viral transmission: A review. *Environmental Chemistry Letters*, *19*(3), 1953–1970. https://doi.org/10.1007/s10311-020-01174-8

Chen, S., Prettner, K., Kuhn, M., Geldsetzer, P., Wang, C., Bärnighausen, T., & Bloom, D. E. (2021). Climate and the spread of COVID-19. *Scientific Reports*, *11*(1), 1–6. https://doi.org/10.1038/s41598-021-87692-z

Choi, Y., Tuel, A., & Eltahir, E. A. B. (2021). *On the environmental Determinants of COVID-19 seasonality*. GeoHealth 5.

CNECovid. (2021). *CNECovid*. Retrieved from https://cnecovid.isciii.es/covid19/#documentaci%C3%B3n-y-datos

Conrad, V. (1946). Usual formulas of continentality and their limits of validity. *Eos, Transactions American Geophysical Union*, *27*(5), 663–664. https://doi.org/10.1029/tr027i005p00663

Corbane, C., Florczyk, A., Pesaresi, M., Politis, P., & Syrris, V. (2018). *GHS-BUILT R2018A - GHS built-up grid, derived from Landsat, multi-temporal (1975-1990-2000-2014)*. https://doi.org/10.2905/jrc-ghsl-10007

Corbane, C., Pesaresi, M., Kemper, T., Politis, P., Florczyk, A. J., Syrris, V., et al. (2019). Automated global delineation of human settlements from 40 years of Landsat satellite data archives. *Big Earth Data*, *3*(2), 140–169. https://doi.org/10.1080/20964471.2019.1625528

Corbane, C., Pesaresi, M., Politis, P., Syrris, V., Florczyk, A. J., Soille, P., et al. (2017). Big Earth data analytics on Sentinel-1 and Landsat imagery in support to global human settlements mapping. *Big Earth Data*, *1*(1–2), 118–144. https://doi.org/10.1080/20964471.2017.1397899

Corbane, C., Politis, P., Syrris, V., & Pesaresi, M. (2018). *GHS built-up grid, derived from Sentinel-1 (2016)*, R2018A. https://doi.org/10.2905/jrc-ghsl-10008

Cui, D., Liang, S., & Wang, D. (2021). Observed and projected changes in global climate zones based on Köppen climate classification. *WIREs Climate Change*, *12*(3), e701. https://doi.org/10.1002/wcc.701

D'Amato, G., Cecchi, L., D'Amato, M., & Annesi-Maesano, I. (2014). Climate change and respiratory diseases. *European Respiratory Review*, *23*(132), 161–169. https://doi.org/10.1183/09059180.00001714

Dijkstra, L., Florczyk, A. J., Freire, S., Kemper, T., Melchiorri, M., Pesaresi, M., & Schiavina, M. (2020). Applying the degree of urbanisation to the globe: A new harmonised definition reveals a different picture of global urbanisation. *Journal of Urban Economics*, *125*, 103312. https://doi.org/10.1016/j.jue.2020.103312

Driscoll, D. M., & Yee Fong, J. M. (1992). Continentality: A basic climatic parameter re-examined. *International Journal of Climatology*, *12*(2), 185–192. https://doi.org/10.1002/joc.3370120207

e Almeida, L. d. O., Favaro, A., Raimundo-Costa, W., Anhê, A. C. B. M., Ferreira, D. C., Blanes-Vidal, V., & dos Santos Senhuk, A. P. M. (2020). Influence of urban forest on traffic air pollution and children respiratory health. *Environmental Monitoring and Assessment*, *192*(3), 1–9. https://doi.org/10.1007/s10661-020-8142-4

Ebert, K., Ekstedt, K., & Jarsjö, J. (2016). GIS analysis of effects of future Baltic sea level rise on the island of Gotland, Sweden. *Natural Hazards and Earth System Sciences*, *16*(7), 1571–1582. https://doi.org/10.5194/nhess-16-1571-2016

Ebert, K., Houts, R., & Noce, S. (2022). *Lower COVID-19 incidence in low-continentality west-coast areas of Europe* [Dataset]. . https://doi.org/10.5281/zenodo.5900811

ECDC. (2020). *COVID-19 pandemic situation update [WWW Document] Eur. Cent. Dis. Prev. Control*. Retrieved from https://www.ecdc.europa.eu/en/covid-19-pandemic

Ehlert, A. (2021). The socio-economic determinants of COVID-19: A spatial analysis of German county level data. *Socio-Economic Planning Sciences*, *101083*. https://doi.org/10.1016/j.seps.2021.101083

European Commission. (2021). *Applying the degree of urbanisation: A methodological manual to define cities, towns and rural areas for international comparisons*. Publications Office of the European Union. https://doi.org/10.2785/706535

Eurostat. (2011). *Background - Degree of urbanisation - Eurostat*. [WWW Document] Retrieved from (1.19.22). https://ec.europa.eu/eurostat/web/degree-of-urbanisation/background

Eurostat. (2020). Eurostat. Your key to European statistics. [Dataset]. . [WWW Document]. Retrieved from https://ec.europa.eu/eurostat/web/gisco/geodata/reference-data/administrative-units-statistical-units/

FHM. (2020). *Folkhälsomyndigheten (Public health agency of Sweden): COVID-19 bekräftade fall i Sverige - daglig uppdatering (confirmed cases in Sweden - daily update)*. [WWW Document]. Retrieved from https://www.folkhalsomyndigheten.se/smittskydd-beredskap/utbrott/aktuella-utbrott/covid-19/statistik-och-analyser/bekraftade-fall-i-sverige/

Florczyk, A. J., Corbane, C., Ehrlich, D., Freire, S., Kemper, T., Maffenini, L., et al. (2019). *GHSL data package 2019: Public release GHS P2019*.

Folkhälsomyndigheten (2021). https://www.folkhalsomyndigheten.se/smittskydd-beredskap/utbrott/aktuella-utbrott/covid-19/statistik-och-analyser/bekraftade-fall-i-sverige/

Forkel, M. (2015). *Das Klima der Erde | Effektive Klimaklassifikation (Köppen)*. [WWW Document]. Retrieved from http://klima-der-erde.de/koeppen.html

Franch-Pardo, I., Napoletano, B. M., Rosete-Verges, F., & Billa, L. (2020). Spatial analysis and GIS in the study of COVID-19. A review. *The Science of the Total Environment*, *739*, 140033. https://doi.org/10.1016/j.scitotenv.2020.140033

Geiger, R. (1954). Landolt-Börnstein – Zahlenwerte und Funktionen aus Physik, Chemie, Astronomie, Geophysik und Technik, alte Serie Vol. 3. *Ch. Klassifikation der Klimate nach W. Köppen*, Springer. (pp. 603–607).

Github (2021). *Covid data Italy*. Retrieved from https://github.com/pcm-dpc/COVID-19/tree/master/dati-province

González-Val, R., & Sanz-Gracia, F. (2021). Urbanization and COVID-19 incidence: A cross-country investigation. *Papers in Regional Science*, *101*, 415. https://doi.org/10.1111/pirs.12647

Haas, E. J., Angulo, F. J., McLaughlin, J. M., Anis, E., Singer, S. R., Khan, F., et al. (2021). Impact and effectiveness of mRNA BNT162b2 vaccine against SARS-CoV-2 infections and COVID-19 cases, hospitalisations, and deaths following a nationwide vaccination campaign in Israel: An observational study using national surveillance data. *The Lancet*, *397*(10287), 1819–1829. https://doi.org/10.1016/s0140-6736(21)00947-8

Hassaan, M. A., Abdelwahab, R. G., Elbarky, T. A., & Ghazy, R. M. (2021). GIS-based analysis framework to identify the determinants of COVID-19 incidence and fatality in Africa. *Journal of Primary Care & Community Health*, *12*, 215013272110412. https://doi.org/10.1177/21501327211041208

Islam, N., Lacey, B., Shabnam, S., Erzurumluoglu, A. M., Dambha-Miller, H., Chowell, G., et al. (2021). Social inequality and the syndemic of chronic disease and COVID-19: County-level analysis in the USA. *Journal of Epidemiology & Community Health*, *75*(6), 496–500. https://doi.org/10.1136/jech-2020-215626

Jensen, M. M. (1964). Inactivation of airborne viruses by ultraviolet irradiation. *Applied Microbiology*, *12*(5), 418–420. https://doi.org/10.1128/am.12.5.418-420.1964

JHUM. (2020). *COVID-19 Dashboard by the center for systems science and Engineering*. (CSSE) at Johns Hopkins University (JHU) [WWW Document]. Coronavirus Resour. Cent. Retrieved from https://coronavirus.jhu.edu/map.html

Kamel Boulos, M. N., & Geraghty, E. M. (2020). Geographical tracking and mapping of coronavirus disease COVID-19/severe acute respiratory syndrome coronavirus 2 (SARS-CoV-2) epidemic and associated events around the world: How 21st century GIS technologies are supporting the global fight against outbreaks and epidemics. *International Journal of Health Geographics*, *19*(1). https://doi.org/10.1186/s12942-020-00202-8

Kashem, S. B., Baker, D. M., González, S. R., & Lee, C. A. (2021). Exploring the nexus between social vulnerability, built environment, and the prevalence of COVID-19: A case study of Chicago. *Sustainable Cities and Society*, *75*, 103261. https://doi.org/10.1016/j.scs.2021.103261

Köppen, W. (1900). Versuch einer Klassifikation der Klimate, vorzugsweise nach ihren Beziehungen zur Pflanzenwelt. *Geographische Zeitschrift*, *6*, 593–611.

Kottek, M., Grieser, J., Beck, C., Rudolf, B., & Rubel, F. (2006). World Map of the Köppen-Geiger climate classification updated. *Meteorologische Zeitschrift*, *15*, (3), 259–263. https://doi.org/10.1127/0941-2948/2006/0130

Kronfeld-Schor, N., Stevenson, T. J., Nickbakhsh, S., Schernhammer, E. S., Dopico, X. C., Dayan, T., et al. (2021). Drivers of infectious disease seasonality: Potential implications for COVID-19. *Journal of Biological Rhythms*, *36*(1), 35–54. https://doi.org/10.1177/0748730420987322

Liu, X., Huang, J., Li, C., Zhao, Y., Wang, D., Huang, Z., & Yang, K. (2021). The role of seasonality in the spread of COVID-19 pandemic. *Environmental Research*, *195*, 110874. https://doi.org/10.1016/j.envres.2021.110874

Loché Fernández-Ahúja, J. M., & Fernández Martínez, J. L. (2021). Effects of climate variables on the COVID-19 outbreak in Spain. *International Journal of Hygiene and Environmental Health*, *234*, 113723. https://doi.org/10.1016/j.ijheh.2021.113723

Loomba, R. S., Aggarwal, G., Aggarwal, S., Flores, S., Villarreal, E. G., Farias, J. S., & Lavie, C. J. (2021). Disparities in case frequency and mortality of coronavirus disease 2019 (COVID-19) among various states in the United States. *Annals of Medicine*, *53*(1), 151–159. https://doi.org/10.1080/07853890.2020.1840620

Luan, H., & Law, J. (2014). Web GIS-based public health surveillance systems: A systematic review. *ISPRS International Journal of Geo-Information*, *3*(2), 481–506. https://doi.org/10.3390/ijgi3020481

Martelletti, L., & Martelletti, P. (2020). Air pollution and the novel Covid-19 disease: A putative disease risk factor. *SN comprehensive clinical medicine*, *2*(4), 383–387. https://doi.org/10.1007/s42399-020-00274-4

Martinez, M. E. (2018). The calendar of epidemics: Seasonal cycles of infectious diseases. *PLoS Pathogens*, *14*(11), e1007327. https://doi.org/10.1371/journal.ppat.1007327

Matthew, O. J., Eludoyin, A. O., & Oluwadiya, K. S. (2021). Spatio-temporal variations in COVID-19 in relation to the global climate distribution and fluctuations. *Spatial and spatio-temporal epidemiology*, *37*, 100417. https://doi.org/10.1016/j.sste.2021.100417

McLafferty, S. L. (2003). GIS and health care. *Annual Review of Public Health*, *24*(1), 25–42. https://doi.org/10.1146/annurev.publhealth.24.012902.141012

Naranjo, L., Glantz, M. H., Temirbekov, S., & Ramírez, I. J. (2018). El Niño and the Köppen–Geiger classification: A prototype concept and methodology for mapping impacts in central America and the Circum-Caribbean. *International Journal of Disaster Risk Science*, *9*(2), 224–236. https://doi.org/10.1007/s13753-018-0176-7

Noce, S., Caporaso, L., & Santini, M. (2019). CMCC-BioClimInd. A new global dataset of bioclimatic indicators. [Dataset]. . https://doi.org/10.1594/PANGAEA.904278

Noce, S., Caporaso, L., & Santini, M. (2020). A new global dataset of bioclimatic indicators. *Scientific Data*, *7*(1), 1–12. https://doi.org/10.1038/s41597-020-00726-5

Nordbø, E. C. A., Nordh, H., Raanaas, R. K., & Aamodt, G. (2018). GIS-derived measures of the built environment determinants of mental health and activity participation in childhood and adolescence: A systematic review. *Landscape and Urban Planning*, *177*, 19–37. https://doi.org/10.1016/j.landurbplan.2018.04.009

Notari, A. (2021). Temperature dependence of COVID-19 transmission. *The Science of the Total Environment*, *763*, 144390. https://doi.org/10.1016/j.scitotenv.2020.144390

Obando-Pacheco, P., Justicia-Grande, A. J., Rivero-Calle, I., Rodríguez-Tenreiro, C., Sly, P., Ramilo, O., et al. (2018). Respiratory syncytial virus seasonality: A global overview. *The Journal of Infectious Diseases*, *217*(9), 1356–1364. https://doi.org/10.1093/infdis/jiy056

Paez, A. (2021). Reproducibility of research during COVID-19: Examining the case of population density and the basic reproductive rate from the perspective of spatial analysis. *Geographical Analysis*. https://doi.org/10.1111/gean.12307

Pesaresi, M., Florczyk, A., Schiavina, M., Melchiorri, M., & Maffenini, L. (2019). GHS-SMOD R2019A - GHS settlement layers, updated and refined REGIO model 2014 in application to GHS-BUILT R2018A and GHS-POP R2019A, multitemporal (1975-1990-2000-2015). *European Commission, Joint Research Centre (JRC)*. [Dataset]. Retrieved from http://data.europa.eu/89h/42e8be89-54ff-464e-be7b-bf9e64da5218

Piazzola, J., Bruch, W., Desnues, C., Parent, P., Yohia, C., & Canepa, E. (2021). Influence of meteorological conditions and aerosol properties on the COVID-19 contamination of the population in coastal and continental areas in France: Study of offshore and onshore winds. *Atmosphere*, *12*(4), 523. https://doi.org/10.3390/atmos12040523

Prata, D., Rodrigues, W., De Souza Bermejo, P. H., Moreira, M., Camargo, W., Lisboa, M., et al. (2021). The relationship between (sub) tropical climates and the incidence of COVID-19. *PeerJ*, *9*, e10655. https://doi.org/10.7717/peerj.10655

Rader, B., Scarpino, S. V., Nande, A., Hill, A. L., Adlam, B., Reiner, R. C., et al. (2020). Crowding and the shape of COVID-19 epidemics. *Nature Medicine*, *26*(12), 1829–1834. https://doi.org/10.1038/s41591-020-1104-0

Ritchie, H., Ortiz-Ospina, E., Beltekian, D., Mathieu, E., Hasell, J., Macdonald, B., et al. (2020). Our world in data. Coronavirus Pandemic (COVID-19) [WWW Document]. OurWorldInData.org. Retrieved from https://ourworldindata.org/coronavirus

Robert Koch Institut. (2020). *Robert Koch Institut. Web-based query on data reported under the German "Protection against infection act" [WWW Document]*. Retrieved from https://survstat.rki.de/

Rojo, J., Picornell, A., Oteros, J., Werchan, M., Werchan, B., Bergmann, K.-C., et al. (2021). Consequences of climate change on airborne pollen in Bavaria, Central Europe. *Regional Environmental Change*, *21*(1), 1–13. https://doi.org/10.1007/s10113-020-01729-z

Sagripanti, J., & Lytle, C. D. (2020). Estimated Inactivation of Coronaviruses by Solar Radiation With Special Reference to COVID-19. *Photochem Photobiol*, *96*, 731–737. https://doi.org/10.1111/php.13293

Santini, M., & di Paola, A. (2015). Changes in the world rivers' discharge projected from an updated high resolution dataset of current and future climate zones. *Journal of Hydrology*, *531*, 768–780. https://doi.org/10.1016/j.jhydrol.2015.10.050

Schiavina, M., Melchiorri, M., & Freire, S. (2019). *GHS_DUC R2019A - GHS Degree of Urbanisation Classification* (Vol. 2000, p. 1990). https://doi.org/10.2905/ED8E8E11-62C3-4895-A7B9-5EF851F112ED

Sera, F., Armstrong, B., Abbott, S., Meakin, S., O'Reilly, K., von Borries, R., et al. (2021). A cross-sectional analysis of meteorological factors and SARS-CoV-2 transmission in 409 cities across 26 countries. *Nature Communications*, *12*(1), 1–11. https://doi.org/10.1038/s41467-021-25914-8

Shaman, J., & Kohn, M. (2009). Absolute humidity modulates influenza survival, transmission, and seasonality. *Proceedings of the National Academy of Sciences*, *106*(9), 3243–3248. https://doi.org/10.1073/pnas.0806852106

Sharmeen, F., Arentze, T., & Timmermans, H. (2014). Dynamics of face-to-face social interaction frequency: Role of accessibility, urbanization, changes in geographical distance and path dependence. *Journal of Transport Geography*, *34*, 211–220. https://doi.org/10.1016/j.jtrangeo.2013.12.011

Tamerius, J. D., Shaman, J., Alonso, W. J., Bloom-Feshbach, K., Uejio, C. K., Comrie, A., & Viboud, C. (2013). Environmental predictors of seasonal influenza epidemics across temperate and tropical climates. *PLoS Pathogens*, *9*(3), e1003194. https://doi.org/10.1371/journal.ppat.1003194

Torregrosa, A., Taylor, M. D., Flint, L. E., & Flint, A. L. (2013). Present, future, and novel bioclimates of the san Francisco, California region. *PLoS One*, *8*(3), e58450. https://doi.org/10.1371/journal.pone.0058450

VG. (2021). *Based on data from Folkehelseinstituttet* (Norwegian Institute of Public Health). Retrieved from https://www.fhi.no/

Yang, S. Q., & Matzarakis, A. (2016). Implementation of human thermal comfort information in Köppen-Geiger climate classification—The example of China. *International Journal of Biometeorology*, *60*(11), 1801–1805. https://doi.org/10.1007/s00484-016-1155-6